Cuttings transport with drillstring rotation

Problem presented by

Paul Bolchover

Schlumberger

Problem statement

When an oil well is being drilled, rock cuttings are transported up to the surface by a flow of viscous non-Newtonian fluid. Current mathematical models of the flow and transport neglect the effects of drillstring rotation. Schlumberger wish to have a model that includes these effects. The Study Group identified many of the ingredients that need to go into building such a model.

Study Group contributors

David Allwright (Smith Institute)
Clare Bailey (Loughborough University)
Chris Cawthorn (DAMTP)
Andrew Cliffe (University of Nottingham)
Erhan Coskun (Trabzon)
Stephen Hibberd (University of Nottingham)
Gareth Jones (OCIAM)
John King (University of Nottingham)
Andrew Lacey (Heriot-Watt)
Rafael Morones (Mexico)
John Ockendon (OCIAM)
Giles Richardson (University of Nottingham)
Hannah Woollard (University of Nottingham)

Report prepared by

David Allwright (Smith Institute), Claire Bailey (Loughborough University),
Chris Cawthorn (DAMTP), Andrew Lacey (Heriot-Watt)

1   Introduction

When an oil well is drilled, it is necessary to transport the rock cuttings up to the surface. To do this, fluid is pumped down through the centre of the drillstring, through nozzles in the bit, and back up to the surface in the annular gap between the drillstring and the drilled hole as illustrated in Figure 1. This fluid is a polymer solution, viscous, shear-
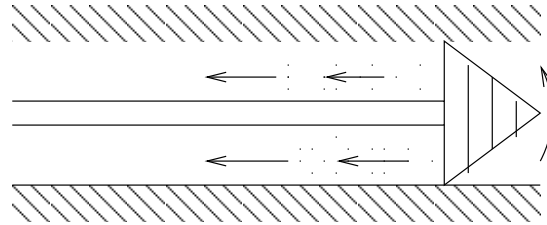

Figure 1: Schematic of rotation and flow in horizontal drilling

thinning, and will typically have a gel strength. The flow in the annular region may be laminar or turbulent. The wellbore may have long sections that are approximately horizontal, in which a bed of cuttings may form at the bottom of the annulus. The drillstring is rotating, and generally off-centre because of its weight, and influences the flow significantly: the rotational velocity of the drillstring and the axial velocity of the fluid are comparable. Schlumberger have a reasonable mechanical model for the transport of rock cuttings when there is no drillstring rotation, and wish to know how this model needs to be modified or replaced to incorporate the effects of rotation. These models are based on work in the published literature, and involve assuming that the cross-section consists of some cuttings in a static bed and some in suspension as illustrated in Figure 2 on the left, with the possibility also of a sliding bed of cuttings as in the centre diagram. However, with rotation we may expect the cross-section of the cuttings bed to be more as shown on the right.
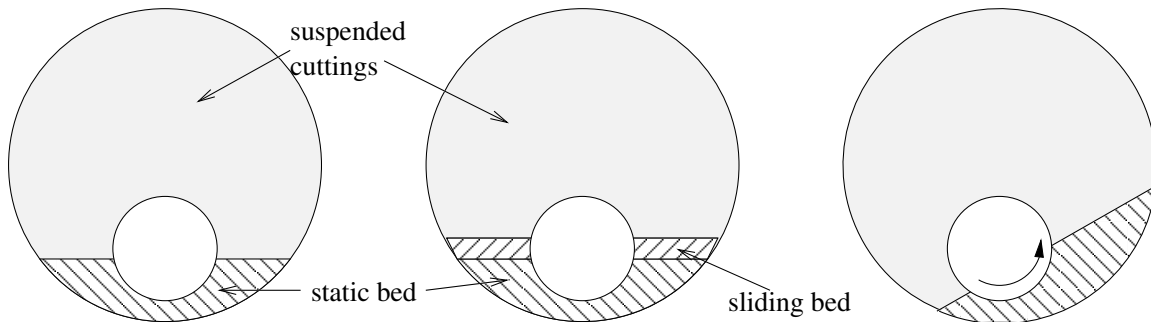

Figure 2: Suspension and rock cuttings bed without rotation (left and centre) and with rotation (right).

Figure 3 comes from a cleaning video made by MI HDD Mining and Waterwell, a company in Houston, Texas. The figure is a still from the video showing fluid (in yellow) flowing up an inclined pipe, and carrying in with it some particles (in black). Inside the fluid is the drill string, which cannot be seen, but which is able to rotate at approximately

Figure 3: Still taken from a video made by MI HDD Mining and Waterwell. It shows fluid (yellow) moving up a pipe, entraining some particles (black) from the bed so they are suspended in the fluid.

150 rpm. The video demonstrates that fluid flowing in a channel where the drillpipe is off-centre suspends more of the particles, and in many cases, does not allow a bed to form at all.

Models of rock cuttings transport are important to help avoid operating in regimes where a heavy bed of cuttings builds up, since there is then the risk that the drillstring will become stuck. A stuck pipe is very expensive and time-consuming to clear. Some of the existing approaches to modelling cuttings transport are described in the references here, and in particular in [2] and [9].[1] A model for cuttings transport over the length of the pipe requires us to have a model for the rate of transport at each point as a function of the local conditions, and therefore in particular a model of the local flow regime. So the questions addressed by the Study Group were

- Under what rotational conditions does a bed form?

- What is the steady-state bed thickness, and is this small enough not to clog up the pipe?

2 Basic data and approaches

The outer diameter of the hole may be about 10 cm, the drillstring diameter up to 5 cm, and the rotation rate about 60 rpm, but of course all of these can vary depending on the equipment used. We shall use notation and representative orders of magnitude from the table below.

---

[1]One question asked at the Study Group was where the model $\tau_s = [h_s(\rho_s - \rho_f)gV_{bsh}]\tan\phi$, [9, equation (7), corrected] comes from, where h_s is the thickness of a dispersed horizontal layer consisting of grains of density ρ_s with volume fraction V_{bsh} in fluid of density ρ_f, when the shear stress at the top of the layer is τ_s and the dynamic contact angle is ϕ. In fact, it arises by thinking of $\tan\phi$ as the dynamic coefficient of friction, the quantity in [.] as the normal pressure stress between the grains in the dispersed layer and the stationary grains below, and using the fact that in steady flow the shear stresses at the top and bottom of the layer are equal.

hole diameter	r_0	$O(10^{-1})\,\mathrm{m}$
drillstring radius	r_1	$O(10^{-1})\,\mathrm{m}$
rotation rate	ω	$O(10)\,\mathrm{rad/s}$
axial velocity	v_z	$O(1)\,\mathrm{m/s}$
fluid density	ρ_f	$O(10^3)\,\mathrm{kg/m^3}$
fluid effective viscosity	μ_f	$O(10^{-2})\,\mathrm{Pa\ s}$
particle radius	a_p	$O(10^{-3})\,\mathrm{m}$
particle density	ρ_p	$O(10^3)\,\mathrm{kg/m^3}$
particle mass	$m \propto \rho_p a_p^3$	$O(10^{-6})\,\mathrm{kg}$

The Reynolds number for the rotational flow is estimated as

$$\mathrm{Re}_\omega = \frac{\rho_f \omega r_0^2}{\mu_f} = O(10^4), \tag{1}$$

and for axial flow the Reynolds number can be up to

$$\mathrm{Re}_z = \frac{\rho_f v_z r_0}{\mu_f} = O(10^4). \tag{2}$$

The Reynolds number for an individual rock cutting particle is

$$\mathrm{Re}_p = \frac{\rho_f \omega r_0 a_p}{\mu_f} = \left(\frac{a_p}{r_0}\right)\mathrm{Re}_\omega = O(10^2). \tag{3}$$

The models we shall consider will be first for a dilute suspension with no bed, in Section 3, then a thin bed with Couette-type flow between the drillstring and bed in Section 4, and finally a thick bed with lubrication flow in a thin layer between the drillstring and the bed in Section 5.

In this report we consider only the rotational flow, not the axial flow. In general terms, the effect of the combination of axial and rotational flow will be that the velocity of the fluid over a cuttings bed will be greater than for either flow alone, and so the increased shear on the cuttings bed will increase the take-up of cuttings into suspension. However, the details of the interaction between the axial and circumferential flows were not studied at the Study Group.

3 Dilute suspensions

When the rock cuttings are a dilute suspension in the flow, we neglect interaction forces between the particles, treat the fluid flow as unaffected by the particles, and then compute particle paths.

Thus the first step is to compute the fluid flow and this depends on the eccentricity of the annular region, and the rotation rate and fluid rheology. We define the eccentricity of the region shown in Figure 4 as $e = r_2/(r_0 - r_1)$ so that $e = 0$ is the concentric case and $e \to 1$ when the drillstring approaches the wall. Figure 5 shows the streamlines
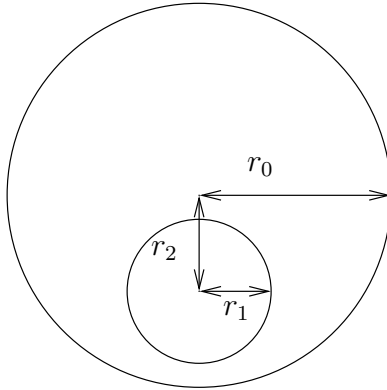
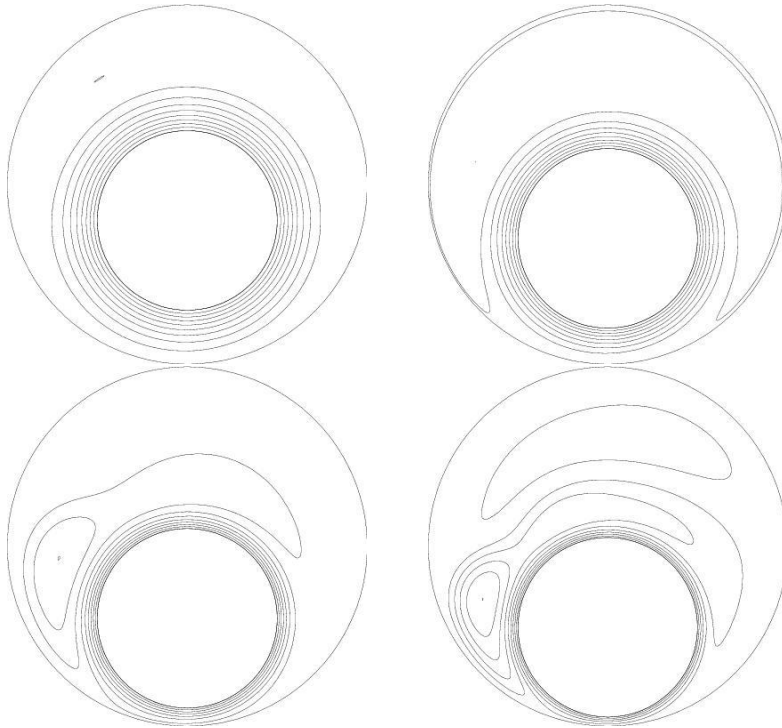Figure 4: Definition of eccentricity $e = r_2/(r_0 - r_1)$.

Figure 5: Particle trajectories for $r_1 = r_0/2$ for eccentricities $e = 0.4, 0.6, 0.8, 0.9$, all for a rotational Reynolds number $\mathrm{Re}_\omega = 10^3$.

for a Newtonian fluid at rotational Reynolds number 10^3, in annuli with $r_1 = r_0/2$ for eccentricities $e = 0.4, 0.6, 0.8, 0.9$, obtained using finite elements. It is clear that for a more eccentric drillstring there can be a primary flow cell driven directly by the rotation, and a secondary recirculating cell above. The effect of such a flow on small particle transport is, in general terms, that particles are convected with the flow, and there is a slower transport of particles across the streamlines by inertia and gravity.

In detail, the motion of a particle of mass m is determined by

$$m\frac{d^2\mathbf{x}}{dt^2} = (\text{Drag force}) + m\mathbf{g}. \tag{4}$$

The drag force will depend on the particle Reynolds number Re_p and when Re is not too large we could take

$$(\text{Stokes' drag}) = k\left(\mathbf{V}(\mathbf{x}) - \frac{d\mathbf{x}}{dt}\right), \tag{5}$$

where $k = 6\pi a_p \mu_f$ for a spherical particle of radius a_p in Newtonian fluid of dynamic viscosity μ_f. Alternatively, for higher Reynolds' numbers we would use the inertial drag of the form

$$(\text{Inertial drag}) = C_D \pi a_p^2 \rho_f \left|\mathbf{V}(\mathbf{x}) - \frac{d\mathbf{x}}{dt}\right|\left(\mathbf{V}(\mathbf{x}) - \frac{d\mathbf{x}}{dt}\right), \tag{6}$$

where ρ_f is the fluid density and C_D the drag coefficient. In each of these, $\mathbf{V}(\mathbf{x})$ is the steady velocity in the rotating flow. Since we estimate these drag forces to be of comparable size in the problem in question, we shall in fact use the Stokes' form (5) for simplicity in the calculations. When we scale $\mathbf{x}$ by r_0 and t by $1/\omega$ we have

$$\epsilon\frac{d^2\mathbf{x}}{dt^2} + \frac{d\mathbf{x}}{dt} = \mathbf{V}(\mathbf{x}) - \epsilon g_0 \mathbf{j}, \tag{7}$$

where $\mathbf{j}$ is a unit vector vertically upwards, and the dimensionless parameters are

$$\epsilon = m\omega/k = \omega t_a \propto \frac{(\text{acceleration time})}{(\text{rotation time})} = O(10^{-1}) \tag{8}$$

$$g_0 = \frac{g}{\omega^2 r_0} \propto \frac{(\text{gravity})}{(\text{centrifugal acceleration})}. \tag{9}$$

Here the acceleration time $t_a = m/k$ is the time-constant for the particle to reach equilibrium with the surrounding flow, so ϵ can be thought of as the Stokes number for the particle. Since ϵ is of order 10^{-1}, particles reach equilibrium with the flow in a time much shorter than the rotation period.

3.1   Asymptotic analysis in the concentric case

In the concentric case $(e = 0)$ we can pursue this analysis further. Using polar coordinates in the hole cross-section we have

$$\epsilon\left(\frac{d^2r}{dt^2} - r\left(\frac{d\theta}{dt}\right)^2, r\frac{d^2\theta}{dt^2} + 2\frac{d\theta}{dt}\frac{dr}{dt}\right) + \left(\frac{dr}{dt}, r\frac{d\theta}{dt}\right) = (0, rf(r)) - \epsilon g_0(\sin\theta, \cos\theta), \tag{10}$$

where we have let the circumferential velocity be $rf(r)$, so that $f(r)$ is the angular velocity at radius r. With our scaling of the variables we shall have

$$f(r) = \frac{\alpha(1 - r^2)}{r^2}, \quad \text{where} \quad \alpha = \frac{a^2}{1 - a^2}, \quad a = \frac{r_1}{r_0} = \frac{\text{(drillstring radius)}}{\text{(hole radius)}}. \tag{11}$$

The leading order solution is simply rotation with the flow, and to reveal more detail we introduce a slow time scale $\tau = \epsilon t$, and write

$$r = r(\tau, t) \sim r_0 + \epsilon r_1 + \dots, \qquad \theta = \theta(\tau, t) \sim \theta_0 + \epsilon \theta_1 + \dots. \tag{12}$$

The leading order behaviour is then given by

$$r_0 = r_0(\tau), \qquad \frac{\partial \theta_0}{\partial t} = f(r_0), \tag{13}$$

and at next order we have

$$-r_0 \left(\frac{\partial \theta_0}{\partial t} \right)^2 + \frac{\partial r_1}{\partial t} + \frac{dr_0}{d\tau} = -g \sin \theta_0, \tag{14}$$

from which we find

$$\frac{dr_0}{d\tau} = r_0 f(r_0)^2. \tag{15}$$

At large times the particle therefore approaches the wall, and the approach behaviour is described by

$$r_0 \sim 1 - A/\tau, \quad \text{where} \quad A = \frac{1}{4\alpha^2} = \frac{(1 - a^2)^2}{4a^4}. \tag{16}$$

This analysis reveals only the effects of rotation and inertia, not gravity. The effects of gravity are important on a longer timescale, for which we may therefore assume the particle is already near the wall. To analyse the motion in this regime we introduce a new fast time scale $S = \epsilon^{1/2}t$, new slow time scale $T = \epsilon S$, and rescaled radial coordinate R defined by

$$r = 1 - \epsilon^{1/2}R, \quad t = \epsilon^{-1/2}S = \epsilon^{-3/2}T. \tag{17}$$

Then the equations for the force balance at leading order are

$$\frac{\partial \theta_0}{\partial S} = 2\alpha R_0, \quad \frac{\partial R_0}{\partial S} = g_0 \sin \theta_0. \tag{18}$$

These represent the periodic motion in which a particle moves around in the region $r = 1 - O(\epsilon^{1/2})$, being closest to the wall at $\theta = 0$, $r = 1 - \epsilon^{1/2}R^*(T)$ and furthest from it at $\theta = \pi$. To go further we take asymptotic expansions of the form

$$R \sim R_0 + \epsilon^{1/2}R_1 + \epsilon R_2 + \dots \tag{19}$$
$$\theta \sim \theta_0 + \epsilon^{1/2}\theta_1 + \epsilon \theta_2 + \dots, \tag{20}$$

and the equations for the force balance at successive orders are

$$\frac{\partial \theta_1}{\partial S} - R_0 \frac{\partial \theta_0}{\partial S} = -g_0 \cos \theta_0 + \alpha(2R_1 + R_0^2) \tag{21}$$

$$\frac{\partial R_1}{\partial S} = g_0 \theta_1 \cos \theta_0 \tag{22}$$

$$\frac{\partial \theta_2}{\partial S} + \frac{\partial \theta_0}{\partial T} - R_0 \frac{\partial \theta_0}{\partial s} - R_1 \frac{\partial \theta_0}{\partial S} = g_0 \theta_1 \sin \theta_0 + \alpha(2R_2 + 2R_0 R_1 + R_0^3) \tag{23}$$

$$\frac{\partial R_2}{\partial S} + \frac{\partial R_0}{\partial T} + \left(\frac{\partial \theta_0}{\partial S}\right)^2 = \theta_2 \cos \theta_0 - \frac{1}{2}\theta_1^2 \sin \theta_0. \tag{24}$$

It will be this last equation that governs the long term behaviour of $R^*(T)$, and hence of the closest point of approach to the wall. A similar approach could be taken numerically for other computed flows in place of the circular streamlines studied here.

An alternative model to use in this context is for c, the volume density of particles, and the volume flux $\mathbf{q} = c\mathbf{V}(\mathbf{x})$. Assuming concentration is constant along the streamlines ($r = $ constant) and varying across them, in a suitable scaling this model would take the form

$$\frac{\partial c}{\partial \tau} + \frac{\partial}{\partial r}(rf(r)^2 c) = 0. \tag{25}$$

This could be applied to other streamline patterns. Special consideration would need to be given to cases where there is a region of recirculating flow separated from the primary flow by a dividing streamline. Diffusion of particles across the streamlines could be added in on the right here if required, giving a convection-diffusion model.

3.2 Numerical results

Figure 6 shows some three-dimensional particle trajectories computed for one eccentricity and various rotation rates, showing the particle motion out to the wall.

4 Thin bed of cuttings

Here we consider the case where there is a thin bed of rock cuttings on the wall of the hole, as illustrated in Figure 7. In this case, the fluid flow in the suspension above the bed will be taken to be a modified Couette flow, and this will have to be coupled to the bed dynamics. There will be a no-slip condition at the pipe, and then some model will have to be assumed for the bed motion itself, possibly treating it as a viscous fluid with an appropriate effective viscosity, in which case it would also sustain a flow similar to Couette flow. At the interface of the cuttings bed with the suspension one would then have to write down an entrainment model to determine the entrainment and settling rates, and the steady shape of the bed would be determined by balancing the flows. The entrained particles would be assumed to move as described previously for a dilute suspension. This approach was not pursued in further detail.
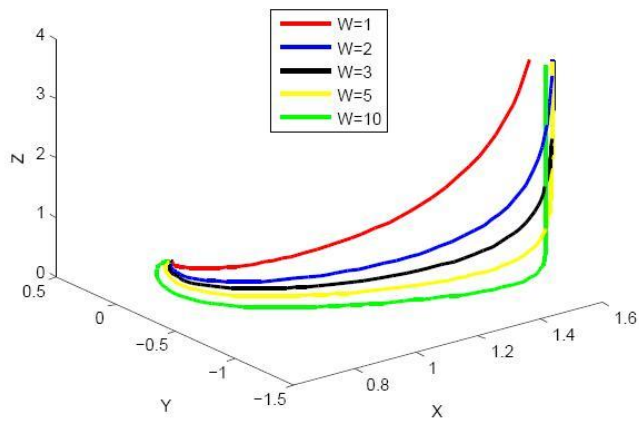
Figure 6: Particle trajectories for different angular velocities, ω (alias W). The z-axis represents the axial direction along the pipe.
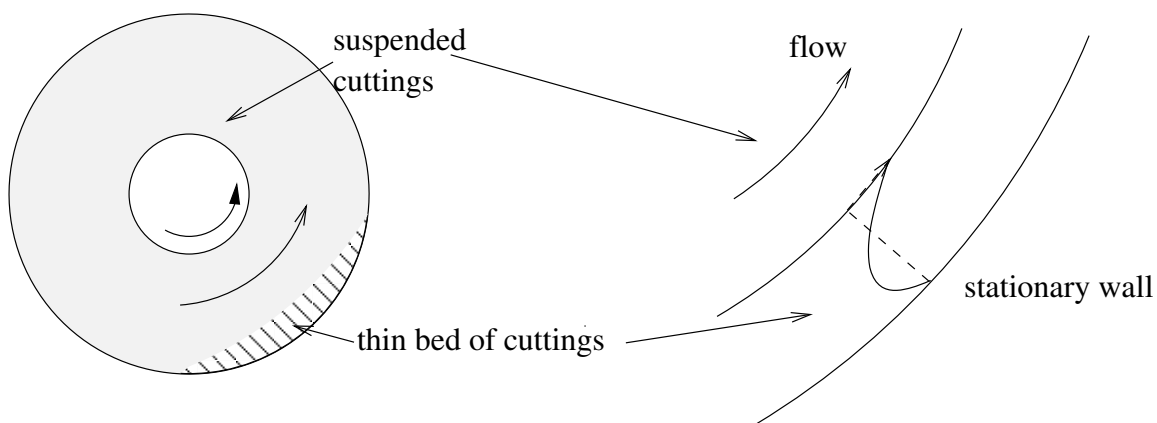

Figure 7: Diagram for the thin bed model. The close-up on the right illustrates the expected velocity profile in the bed.

5 Thick layer model

When the cuttings bed is thick enough that the drillstring lies effectively within it, we need a different model for the fluid flow because the gap between the bed and the drillstring is now much narrower than illustrated in Figure 7. We shall need instead to use lubrication theory for the flow in the gap, and we expect some of the fluid above the drillstring to be in a weak recirculating flow that never enters the gap, roughly as illustrated in Figure 8. The main particle entrainment will occur in the narrow gap, because of the high shear caused by the proximity of the rotating drillstring.
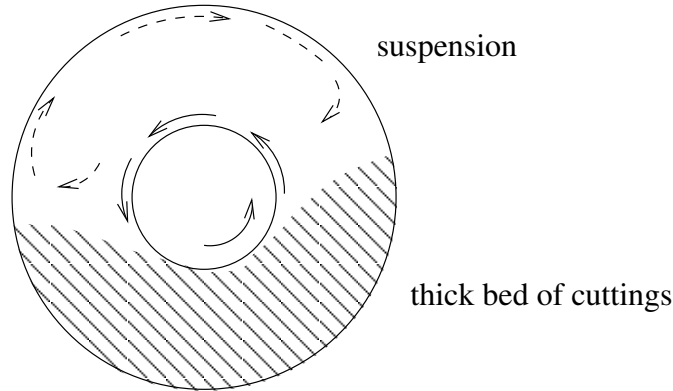

Figure 8: Illustration of flow with a thick bed of rock cuttings.

Although the use of a convection-diffusion model was suggested in the case of a thick bed, or a two-phase flow model, the Study Group work centred on modelling the bed as a granular medium.

5.1 Granular flow model

Consider the particle bed as a two-dimensional strip, with the z-axis in the vertical direction. If we think of this as the narrowest point of the gap then the separation is $L = r_0 - r_1 - r_2$. The particle bed occupies the region of the strip from $z = 0$ (at the earth/rock) to some point $z = h$. At $z = L$ there is the rotating drill string, which is now modelled as a plate above the fluid, moving with velocity $U = r_1 \omega$. As seen in Figure 9, the width of the fluid region is $L - h = \delta \ll L$.

The fluid is modelled as shear-thinning with a gel strength so

$$\tau_{xz} = \tau_0 + K \left(\frac{\partial u}{\partial z} \right)^n. \tag{26}$$

A suitable model for the granular bed is that of Jop *et al.*[7], which takes the form

$$\tau = \mu(I)P \tag{27}$$

where the effective pressure in the granular bed is

$$P = P_0 + \Delta \rho g (h - z), \qquad \Delta \rho = \rho_p - \rho_f. \tag{28}$$
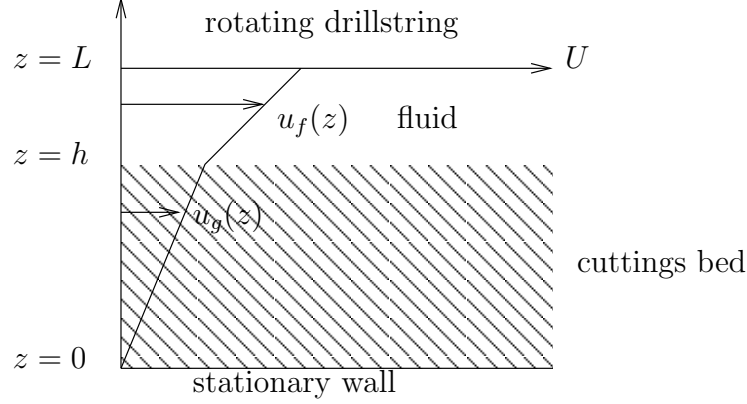
Figure 9: Schematic of rotating drillstring modelled as a strip. Fluid is assumed to flow in the small gap between the particle bed and the rotating drillstring.

The effective friction coefficient is modelled as

$$\mu(I) = \mu_1 + \frac{\mu_2 - \mu_s}{1 + I_0/I}, \tag{29}$$

where

$$I = d \left| \frac{\partial u}{\partial z} \right| \left(\frac{\phi p}{\rho_p} \right)^{-1/2}. \tag{30}$$

In steady flow as illustrated in Figure 9, the velocities of the fluid, $u_f(z)$, and the granular bed, $u_g(z)$, and the grain pressure $P_g(z)$ are given by the expressions

$$u_f(z) = U + \left(\frac{A_0 - \tau_0}{k} \right)^{1/n} (z - L),$$

$$u_g(z) = \frac{2I_0}{\Delta \rho g d} \left[\frac{1}{3} P^{3/2} - (\lambda - 1) D^2 P^{1/2} + \frac{(\lambda - 1) D^3}{2} \log \left| \frac{P^{1/2} + D}{P^{1/2} - D} \right| \right]_{P=P_g(0)}^{P=P_g(z)},$$

$$P_g(z) = P_0 + \Delta \rho g (h - z),$$

where $\lambda = \mu_s/\mu_2 < 1$, $D = \mu_s^2 A_0$, $A_0 = \mu(I)P$, $d = 2a_p$ is the particle diameter, ϕ the volume fraction of solid, and p the pressure.

An empirical entrainment rate, E, will be needed to determine the mass flux from the particle bed to the fluid, and a suitable model [6] is

$$E = \frac{AZ}{1 + \frac{A}{0.3} Z^5}, \qquad \text{where} \qquad Z = \frac{|\mathbf{u} \wedge \mathbf{n}| R_p^n}{v_s},$$

for $n \approx 0.6$. From [6], $A = 1.3 \times 10^7$, although this is material-dependent.

6 Further remarks and conclusions

Although no models are readily available for the whole of this problem, many of the necessary ingredients have been identified. Schlumberger believe that the flow for a

given cutting density and drillstring position can show hysteresis, *i.e.* there can be two stable flow regimes (perhaps a suspended flow and one with a bed) and the actual flow regime obtained in practice will depend on the past history. In such a case we can expect that there will be points along the length of the bore at which the regime changes, and the motion of those points themselves will be critical for the global behaviour. We have not attempted to model such points or their motion, or analyse the transitions between multiple stable behaviours. Instead we have written down models that would be needed for the different flow regimes in order to predict entrainment rates and bed flow. All the models will need to use some empirical law (of which there are many) to write the entrainment rate as a function of the transverse velocity and the shear stress at the fluid-grains interface. Then laws for the particle motion in both the fluid and the bed need to be used to find the equilibrium position and shape of the bed. The granular material model of Jop *et al.*[7] is suggested for the cuttings bed. One area where we have not here suggested any particular model is in the diffusive transport of the suspended cuttings.

References

[1] B.Y.Ballal and R.S.Rivlin. Flow of a Newtonian fluid between eccentric rotating cylinders: inertial effects. Archive for Rational Mechanics and Analysis, 1976.

[2] P.Bolchover. Layer modeling for cuttings transport (without rotation). Handout at Study Group, 2007.

[3] S.F.Chien. Settling velocity of irregularly shaped particles. SPE Drilling and Completion, 281–289, 1994.

[4] Hyun Cho, Subhash N. Shah, Samuel O. Osisanya. A three-layer modeling for cuttings transport with coiled tubing horizontal drilling. SPE 63269, 2000.

[5] Hyun Cho, Subhash N. Shah, Samuel O. Osisanya. A three-segment hydraulic model for cuttings transport in horizontal and deviated wells. SPE 65488, 2000.

[6] M.H.García and G.Parker. Entrainment of Bed Sediment into Suspension. ASCE Journal of Hydraulic Engineering **117**, 414–435, 1991.

[7] P.Jop, Y.Forterre and O.Pouliquen. Crucial role of sidewalls in granular surface flows: consequences for the rheology. Journal of Fluid Mechanics **541**, 167–192, 2005.

[8] A.M.Kamp and M.Riviero. Layer modeling for cuttings transport in highly inclined wellbores. SPE 53942, 1999.

[9] D.Nguyen and S.S.Rahman. A three-layer hydraulic program for effective cuttings transport and hole cleaning in highly deviated and horizontal wells. SPE Drilling and Completion, 182–189, 1998.

[10] J.M.Nouri and J.H.Whitelaw. Flow of Newtonian and non-Newtonian fluids in an eccentric annulus with rotation of the inner cylinder. Int. J. Heat and Fluid Flow **18** 236–246, 1997.

[11] Ali A. Pilehvari, J.J.Azar, Siamack A. Shimazi. State-of-the-art cuttings transport in horizontal wellbores. SPE 37079.